Mathematical Models of Synaptic Transmission and Short-Term Plasticity

R. Bertram

Department of Mathematics and Kasha Institute of Biophysics,
Florida State University, Tallahassee, Florida 32306

1 Introduction

The synapse is the storehouse of memories, both short-term and long-term, and is the location at which learning takes place. There are trillions of synapses in the brain, and in many ways they are one of the fundamental building blocks of this extraordinary organ. As one might expect for such an important structure, the inner workings of the synapse are quite complex. This complexity, along with the small size of a typical synapse, poses many experimental challenges. It is for this reason that mathematical models and computer simulations of synaptic transmission have been used for more than two decades. Many of these models have focused on the presynaptic terminal, particularly on the role of Ca^{2+} in gating transmitter release (Parnas and Segel, 1981; Simon and Llinás, 1985; Fogelson and Zucker, 1985; Yamada and Zucker, 1992; Aharon et al., 1994; Heidelberger et al., 1994; Bertram et al., 1996; Naraghi and Neher, 1997; Bertram et al., 1999a; Tang et al., 2000; Matveev et al., 2002). The terminal is where neurotransmitters are released, and is the site of several forms of short-term plasticity, such as facilitation, augmentation, and depression (Zucker and Regehr, 2002). Mathematical modeling has been used to investigate the properties of various plasticity mechanisms, and to refine understanding of these mechanisms (Fogelson and Zucker, 1985; Yamada and Zucker, 1992; Bertram et al., 1996; Klingauf and Neher, 1997; Bertram and Sherman, 1998; Tang et al., 2000; Matveev et al., 2002). Importantly, modeling has in several cases been the motivation for new experiments (Zucker and Landò, 1986; Hochner et al., 1989; Kamiya and Zucker, 1994; Winslow et al., 1994; Tang et al., 2000). In this chapter, we describe some of the mathematical models that have been developed for transmitter release and presynaptic plasticity, and discuss how these models have shaped, and have been shaped by, experimental studies.

R. Bertram: *Mathematical Models of Synaptic Transmission and Short-Term Plasticity*, Lect. Notes Math. **1867**, 173–202 (2005)

2 Neurotransmitter Release is Evoked by Ca^{2+} Influx

Neurotransmitters are packaged into small spherical structures called **vesicles**, which have a diameter of 30–50 nm. A presynaptic terminal may contain tens or hundreds of filled vesicles, but typically only a fraction of these are docked to the membrane and ready to be released. The docking stations are called **active zones**, and the docked vesicles form the **readily releasable pool**. When an electrical impulse reaches the synapse, ion channels selective for calcium ions open and Ca^{2+} enters the terminal. Much of this Ca^{2+} is rapidly bound by buffer molecules, but a significant fraction remains free and can bind to Ca^{2+} acceptors associated with a docked vesicle. This causes the vesicle to fuse with the cell membrane, allowing neurotransmitter molecules to diffuse out of the vesicle and into the small space (the **synaptic cleft**) separating the presynaptic and postsynaptic cells. The signal is passed to the postsynaptic cell when the transmitter molecules bind to receptors in the postsynaptic membrane, inducing a change in its membrane potential.

The key role that Ca^{2+} plays in neurotransmitter release raises two questions. First, what is the nature of the Ca^{2+} acceptors that, when bound, result in vesicle fusion? Second, what is the nature of the Ca^{2+} signal? Much effort has gone into answering these questions. It was shown by Dodge and Rahamimoff (1967) that there is a fourth-power relation between the external Ca^{2+} concentration and transmitter release in a neuromuscular junction, suggesting that each release site contains four Ca^{2+} acceptors. Although the identity of the acceptors is still under investigation, there is much evidence suggesting that the protein synaptotagmin plays such a role (Geppert et al., 1994; Goda, 1997). Once bound, does Ca^{2+} unbind from an acceptor rapidly or slowly once the membrane is repolarized and the Ca^{2+} channels close? Some data suggest the latter, providing a mechanism for short-term synaptic enhancement (Stanley, 1986; Bertram et al., 1996).

The central question regarding the nature of the Ca^{2+} signal is whether vesicle fusion is gated by the Ca^{2+} microdomain formed at the mouth of a single open Ca^{2+} channel, by overlapping microdomains from several open channels, or by Ca^{2+} from a large aggregate of channels. This should depend on the location of the Ca^{2+} acceptors. Are they located close to Ca^{2+} channels so that they respond primarily to the plume of Ca^{2+} at the mouth of an open channel, or are some of the acceptors farther away so that they respond to a spatially averaged Ca^{2+} signal? Questions regarding the influence of Ca^{2+} channel and Ca^{2+} acceptor geometry have been studied largely through mathematical modeling, constrained by experimental studies of the timing of transmitter release and the effects of exogenous Ca^{2+} buffers.

3 Primed Vesicles are Located Close to Ca^{2+} Channels

Once transmitter-filled vesicles have been transported to the terminal membrane, they then dock and are primed for release. It is only the primed vesicles that can fuse following a presynaptic action potential (Südhof, 1995; Rettig and Neher, 2002). Estimates of the number of primed vesicles per active zone vary from 10 for the CA1 region of the hippocampus (Schikorski and Stevens, 1997) to 130 in cat rod photoreceptors (Rao-Mirotznik et al., 1995). Early work by Llinás et al. (1976) demonstrated that a postsynaptic response can occur within 200 µs of an increase in the presynaptic Ca^{2+} current. A subsequent mathematical study indicated that this temporal restriction constrains the vesicle to be within 10's of nanometers of an open Ca^{2+} channel (Simon and Llinás, 1985). A later study of the large chick calyx synapse demonstrated that transmitter release can be evoked by the opening of a single Ca^{2+} channel, and occurs 200–400 µs after the channel opening (Stanley, 1993). Further evidence for the colocalization of channels and vesicles has been provided by studies showing that proteins forming the **core complex** that associates the vesicle with the terminal membrane, e.g. SNAP-25, syntaxin, and synaptotagmin, bind to Ca^{2+} channels in vertebrate synapses (Sheng et al., 1996, 1997; Jarvis et al., 2002). Finally, the high concentration of Ca^{2+} needed to evoke vesicle fusion, 20 µM or more (Heidelberger et al., 1994), can only be achieved if the Ca^{2+} source is located close to the Ca^{2+} acceptors.

4 Reaction-Diffusion Equations

Many models have been developed of Ca^{2+} diffusion in the presynaptic terminal or near the plasma membrane of endocrine cells (Zucker and Stockbridge, 1983; Fogelson and Zucker, 1985; Neher, 1986; Yamada and Zucker, 1992; Klingauf and Neher, 1997; Naraghi and Neher, 1997; Tang et al., 2000; Matveev et al., 2002, 2004). Most of these include mobile Ca^{2+} buffers. Examples of endogenous mobile buffers are calbindin-D28k and calretinin. Examples of exogenous mobile buffers are the Ca^{2+} chelators EGTA and BAPTA, and the fluorescent dye fura-2. The Ca^{2+}-buffer reaction diffusion equations have the form

$$\frac{\partial Ca}{\partial t} = D_c \bigtriangledown^2 Ca + R \tag{1}$$

$$\frac{\partial B}{\partial t} = D_b \bigtriangledown^2 B + R \tag{2}$$

$$\frac{\partial BC}{\partial t} = D_{bc} \bigtriangledown^2 BC - R \tag{3}$$

where Ca is the intraterminal free Ca^{2+} concentration, B is the free buffer concentration, and BC is the concentration of Ca^{2+} bound to buffer. It is assumed here that there is one mobile buffer, but others can be included in

a natural way. The diffusion coefficients of the three species are D_c, D_b, and D_{bc}. The Ca^{2+} binding reaction (R) is given by

$$R = -k^+ BCa + k^- BC \tag{4}$$

where k^+ and k^- are the binding and unbinding rates, respectively. Physiological values for the diffusion coefficients and kinetic rates can be found in Allbritton et al. (1992); Pethig et al. (1989), and Klingauf and Neher (1997). If the buffer diffuses at the same rate whether Ca^{2+} is bound or not ($D_b \approx D_{bc}$), then the total concentration of buffer, $B_T = B + BC$, is described by

$$\frac{\partial B_T}{\partial t} = D_b \bigtriangledown^2 B_T \, . \tag{5}$$

From this, we see that if B_T is initially uniform, then it remains uniform. It is then possible to eliminate (2), replacing (4) with

$$R = -k^+ (B_T - BC)Ca + k^- BC \, . \tag{6}$$

At the boundary (the terminal membrane), Ca^{2+} influx through an open channel is described by

$$D_c \bigtriangledown Ca = i_{Ca}/(2FA) \tag{7}$$

where i_{Ca} is the single channel Ca^{2+} current, F is Faraday's constant, and A is the channel cross-sectional area. More detailed descriptions of the reaction-diffusion equations and their numerical solution can be found in the modeling papers cited earlier and in Smith et al. (2002).

5 The Simon and Llinás Model

One of the earliest models of Ca^{2+} dynamics in the presynaptic terminal was developed by Simon and Llinás (1985). The goal of this modeling study was to determine the spatial and temporal distribution of Ca^{2+} in the squid giant synapse, a common experimental system due to its large size, during and following depolarization of the presynaptic terminal. Unlike several earlier models, the focus was on the Ca^{2+} microdomains that form at open channels.

This study produced three main predictions: (1) The opening of a Ca^{2+} channel results in a **microdomain** where the Ca^{2+} concentration is greatly elevated above the spatial average of the concentration in the terminal (the **bulk Ca^{2+} concentration**). (2) Within a microdomain, the steady-state concentration is achieved very rapidly (<1 μs) relative to the open time of the channel. (3) The macroscopic Ca^{2+} current (I_{Ca}) is not a good determinant of the microscopic distribution of Ca^{2+} in the terminal. It is the microscopic distribution that is most important for transmitter release, given the colocalization of channels and vesicles. Two other important observations were made.

First, stationary buffers have no effect on the steady-state Ca^{2+} concentration in a microdomain, but do influence the time required to reach a steady state. Second, in the vicinity of a channel the Ca^{2+} concentration is roughly proportional to i_{Ca}, the single-channel Ca^{2+} current.

The spatial extent of a microdomain depends greatly on the magnitude of the flux through the open channel, which itself depends on the voltage **driving force**, the difference between the membrane potential and the Ca^{2+} Nernst potential $(V - V_{Ca})$. When V is low (the terminal is hyperpolarized) the probability that a channel is open is small. However, the driving force is large, so the magnitude and extent of a microdomain formed at the rare open channel is large. In contrast, when V is elevated (the terminal is depolarized) the channel open probability is near one, but now the driving force is small. Hence, when V is relatively low there will be few open channels, each producing a large Ca^{2+} microdomain. When V is high there will be many open channels, each producing a small microdomain. In the latter case there could be significant overlap of microdomains, while in the former case this is unlikely to occur.

The importance of thinking in terms of the microscopic Ca^{2+} distribution, rather than in terms of the macroscopic Ca^{2+} current, is demonstrated nicely by an experiment performed in the squid giant synapse by Augustine et al. (1985). Here, the terminal was voltage clamped and the presynaptic current was recorded. The postsynaptic response, postsynaptic current, was measured simultaneously. This was done for test pulses ranging from −33 mV to 57 mV from a holding potential of −70 mV (Fig. 1). In each case, the bulk of the postsynaptic response occurred *after* the membrane potential was returned to its low holding potential. This is in spite of the fact that the time integral of the macroscopic Ca^{2+} current I_{Ca} was larger during the depolarized test pulse than following the return to the holding potential. The reason for this is that during the depolarization Ca^{2+} channels open, but the accompanying Ca^{2+} microdomains are small. When V is returned to its hyperpolarized holding potential the driving force is instantaneously increased, resulting in a rapid spike in I_{Ca}, called a **tail current** (this is not resolved in Fig. 1). Thus, before the channels have a chance to close large microdomains are formed, and these evoke the bulk of the transmitter release.

6 Steady-State Approximations for Ca^{2+} Microdomains

The colocalization of vesicles and Ca^{2+} channels suggests that transmitter release is gated by single or overlapping Ca^{2+} microdomains. This, combined with the calculations from Simon and Llinás that a steady state is achieved rapidly in a microdomain, has motivated two steady-state approximations for the Ca^{2+} concentration in a microdomain. The first, the **excess buffer approximation** (EBA), assumes that mobile buffer is present in excess and

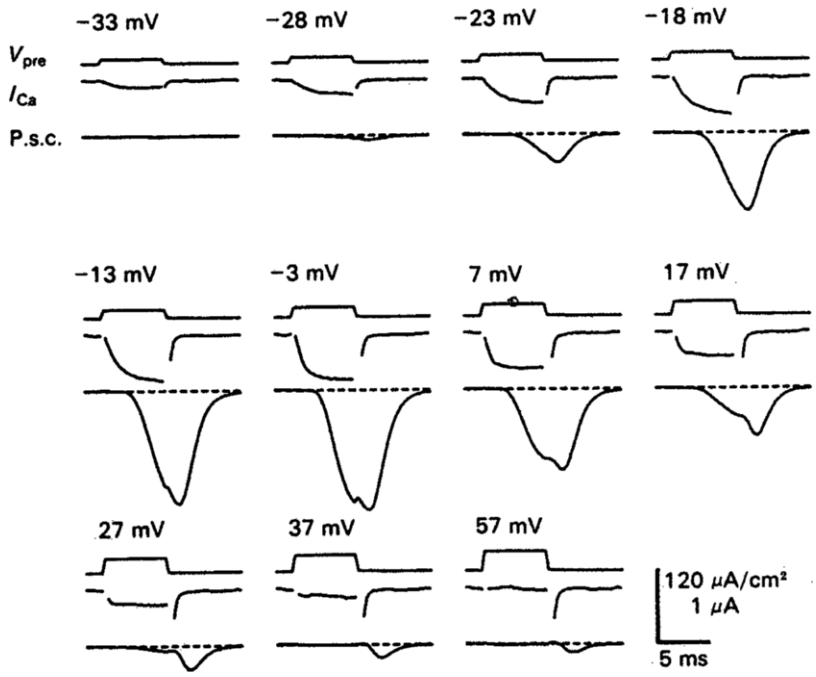

Fig. 1. Recordings of presynaptic Ca^{2+} current (I_{Ca}) and postsynaptic current (P.s.c.) at voltage-clamped terminals (V_{pre}) of the squid giant synapse. Tail currents are not visible. Reprinted with permission from Augustine et al. (1985)

cannot be saturated. It was first derived by Neher (1986), and would be valid, for example, in the saccular hair cell where the endogenous buffer calbindin-D_{28K} is present in millimolar concentrations (Roberts, 1993), or in cells dialyzed with a high concentration of a Ca^{2+} chelator.

The steady-state EBA is:

$$Ca = \frac{\sigma}{2\pi D_c r} e^{-r/\lambda} + Ca_{bk} \tag{8}$$

where σ is the Ca^{2+} flux through an open channel, r is the distance from the channel, and Ca_{bk} is the bulk Ca^{2+} concentration. The parameter λ is the **characteristic length**, which determines the spatial extent of the microdomain. The characteristic length depends on the Ca^{2+} diffusion constant, the buffer binding rate, and the bulk free buffer concentration:

$$\lambda = \sqrt{\frac{D_c}{k^+ B_{bk}}} \,. \tag{9}$$

Figure 2 shows the graph of the EBA for two different values of λ. For the larger λ, the Ca^{2+} concentration is larger at each location and the microdomain has a greater spatial extent. The dependence of λ on D_c and k^+ (or B_{bk})

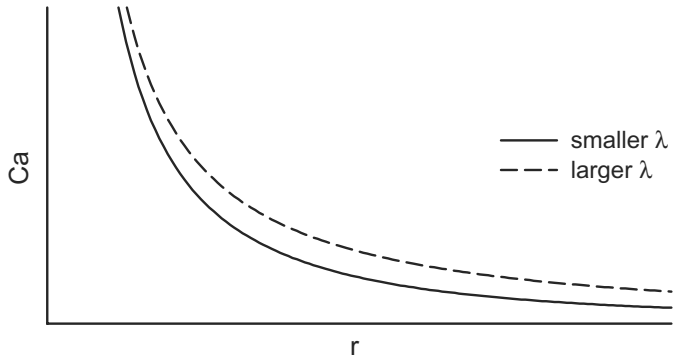

Fig. 2. The steady state Ca^{2+} concentration as a function of distance from an open Ca^{2+} channel, calculated with the EBA (8) using two different values of the characteristic length λ

is illustrated in Fig. 3. The characteristic length increases as the square root of the Ca^{2+} diffusion rate, agreeing with the intuition that the microdomain extends farther when diffusion is more rapid. In contrast, the characteristic length, and the extent of the microdomain, declines when either the buffer binding rate or the buffer concentration is increased.

A second approximation, the **rapid buffer approximation** (RBA), is based on the assumption that the Ca^{2+} buffer is fast compared to the Ca^{2+} diffusion rate (Wagner and Keizer, 1994). This leads to local equilibration, so that at each location the Ca^{2+} and buffer are in equilibrium. Thus,

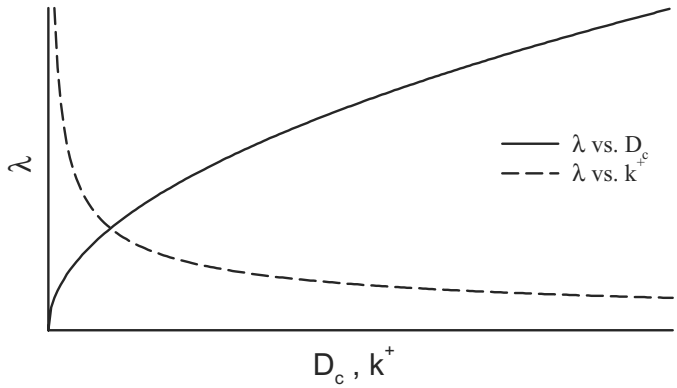

Fig. 3. The dependence of the characteristic length on the Ca^{2+} diffusion coefficient and the buffer binding rate

$$B = \frac{KB_{\text{tot}}}{K + Ca} \tag{10}$$

where K is the dissociation constant ($K = k^-/k^+$) of the buffer. With this approximation, buffer may be saturated when the Ca^{2+} concentration is high, such as near an open Ca^{2+} channel, in contrast with the EBA where buffer does not saturate. Indeed, for the RBA

$$\lim_{r \to 0} B \approx 0 \tag{11}$$

while for the EBA

$$\lim_{r \to 0} B \approx B_{bk} \ . \tag{12}$$

See Smith et al. (2002) for a summary of the two approximations. An asymptotic analysis of the approximations and conditions on their validity is given in Smith et al. (2001).

The steady state RBA was derived by Smith (1996). For a single mobile buffer and a single Ca^{2+} source (channel), it is:

$$Ca = \left(-D_c K + \frac{\sigma}{2\pi r} + D_c Ca_{bk} - D_b B_{bk} + \sqrt{\Omega}\right) \Big/ 2D_c \tag{13}$$

where

$$\Omega = \left(D_c K + \frac{\sigma}{2\pi r} + D_c Ca_{bk} - D_b B_{bk}\right)^2 + 4D_c D_b B_{\text{tot}} K \ . \tag{14}$$

This approximation and the EBA were extended to multiple sources (open channels) in Bertram et al. (1999a).

7 Modeling the Postsynaptic Response

Neurotransmitter molecules released from the presynaptic terminal diffuse across the narrow synaptic cleft (≈20 nm) and can bind to receptors in the postsynaptic cell. These receptors may be linked directly to an ion channel (**ionotropic receptors**) or may activate second messengers, thus providing an indirect link to ion channels (**metabotropic receptors**). We focus here on models of the action of ionotropic receptors, which are simpler than those of metabotropic receptors. For a description of both types of models see (Destexhe et al., 1994).

The postsynaptic membrane contains voltage-gated ion channels that give rise to an ionic current I_{ion}, and ligand-gated channels that give rise to a synaptic current I_{syn}. The postsynaptic voltage V_{post} changes in time according to

$$C_m \frac{dV_{\text{post}}}{dt} = -(I_{\text{ion}} + I_{\text{syn}}) \tag{15}$$

where $I_{\text{syn}} = g_{\text{syn}}(t)(V - V_{\text{syn}})$ and V_{syn} is the reversal potential for the channel (for ionotropic glutamate receptors, for example, $V_{\text{syn}} \approx 0\,\text{mV}$). The time-dependent synaptic conductance g_{syn} has been modeled in two ways: using an α-function and using a kinetic description. The **α-function** was first employed by Rall (1967) to describe the synaptic response in a passive dendrite. It is convenient to write this in terms of dimensionless time, $T = t/\tau_m$, and the dimensionless parameter $\alpha = \tau_m/t_{\text{peak}}$. Here, t is the time after the synaptic event, and t_{peak} is the time after the synaptic event at which g_{syn} reaches its peak value. The parameter $\tau_m = R_m C_m$ is the **membrane time constant** (R_m is the membrane resistance, equal to $1/g_{\text{ion}}$), which determines how rapidly the postsynaptic membrane responds to changes in current. Finally, the synaptic conductance written in terms of the α-function is:

$$g_{\text{syn}}(T) = \bar{g}_{\text{syn}} \alpha T e^{-\alpha T} \tag{16}$$

where $\bar{g}_{\text{syn}}$ is a parameter that sets the size of the response.

Synaptic conductance using (16) is shown following a synaptic event in Fig. 4. Notice the rapid rise and slow fall in conductance that is characteristic of the actual postsynaptic response. We have plotted g_{syn} for two values of the parameter α, demonstrating how doubling α affects the time course of the synaptic conductance. The conductance has been normalized to facilitate comparison of the time courses.

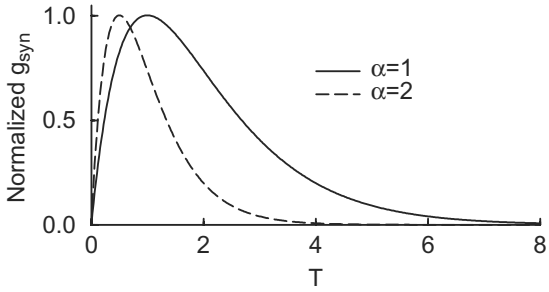

Fig. 4. Normalized synaptic conductance modeled with an α-function. T is the dimensionless time following the synaptic event. Conductance is plotted for two different values of the parameter α

The α-function approach has some disadvantages. First, it does not provide for the summation and saturation of postsynaptic responses. Second, it does not describe receptors/channels with multiple states. An alternative approach is to simulate the postsynaptic response using a kinetic model for the receptor. An excellent description of this approach is given in Destexhe et al. (1994).

The simplest receptor has two states, closed and open, and can be described by the following kinetic scheme:

$$C \underset{\beta}{\overset{\alpha(L)}{\rightleftharpoons}} O$$

where C represents the closed state, O represents the open state, $\alpha(L)$ is the receptor activation rate that depends on the ligand concentration (L), and β is the receptor deactivation rate. Letting O also represent the fraction of activated receptors (or open ionotropic channels) and noting that $1 - O$ is the fraction of non-activated receptors, one can use the law of mass action to obtain:

$$\frac{dO}{dt} = \alpha(1 - O) - \beta O \,, \tag{17}$$

where α and β values for the appropriate receptor type would be used. Then, $g_{\text{syn}}(t) = \bar{g}_{\text{syn}} O$. One would then include (17) with the differential equations describing the postsynaptic voltage and any activation or inactivation variables. A big advantage of this approach is that receptors with complicated kinetics can be readily converted to differential equations and incorporated into the postsynaptic compartment of the model.

8 A Simple Model

In this section the release of transmitter and the postsynaptic response will be demonstrated with a simple model (Bertram, 1997). This model assumes that each releases site is 10 nm from a Ca^{2+} channel, and uses the steady-state RBA for the Ca^{2+} concentration near the channel. Because of the channel colocalization, the stochastic openings and closings of the channel would be reflected in the dynamics of transmitter release. To arrive at a deterministic model, we assume that the release site senses the **average domain Ca^{2+} concentration** rather than the stochastic Ca^{2+} signal from the colocalized channel:

$$\overline{Ca_D} = Ca_D p \tag{18}$$

where Ca_D is the microdomain Ca^{2+} concentration 10 nm from the channel and p is the probability that the channel is open. See Bertram and Sherman (1998) for a discussion of the validity of this deterministic approximation.

It is next assumed that each release site has a single low-affinity Ca^{2+} binding site (the properties of the Ca^{2+} acceptors are discussed later in more detail), with a dissociation constant of 170 μM. The differential equation for the fraction of bound Ca^{2+} acceptors, s, is then:

$$\frac{ds}{dt} = k_s^+ \overline{Ca_D}(1-s) - k_s^- s \tag{19}$$

where $k_s^+ = 0.015\ \text{ms}^{-1}\mu\text{M}^{-1}$ is the Ca^{2+} binding rate and $k_s^- = 2.5\ \text{ms}^{-1}$ is the unbinding rate.

For the postsynaptic response, we assume that the concentration of released transmitter is proportional to the probability of transmitter release (s). We then use a two-state model for the postsynaptic receptor, with fast kinetics and a reversal potential of 0 mV.

The components of neurotransmission simulated with this model are shown in Fig. 5. A presynaptic action potential is generated that peaks at the time indicated by the dashed line (Fig. 5A). During the downstroke of the impulse the Ca^{2+} microdomains are largest (similar to the large tail currents described earlier), so the average domain Ca^{2+} concentration peaks shortly after the peak of the impulse (Fig. 5B). The rise in domain Ca^{2+} causes a spike in the release probability (Fig. 5C), which in turn results in a relatively rapid rise and slow decay in the postsynaptic membrane potential (Fig. 5D). The rapid rise is due to I_{syn}, which is activated during the spike in release probability. The slow decay in V_{post} reflects the membrane properties of the postsynaptic compartment. Thus, we see that the postsynaptic response occurs several milliseconds after the presynaptic impulse, consistent with experimental observations. Also, the postsynaptic potential outlasts the presynaptic signal that initiated it. This allows the postsynaptic potential to summate during a train of presynaptic impulses (Fig. 6).

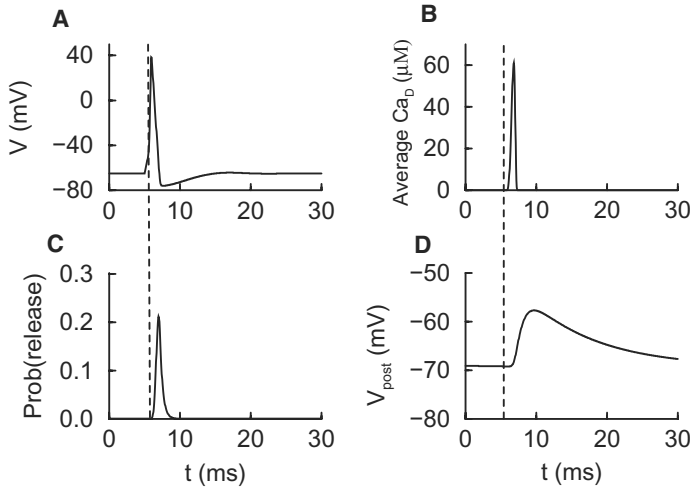

Fig. 5. Simulation of transmitter release and a postsynaptic response. The postsynaptic response is delayed several milliseconds from the presynaptic impulse, and it is longer lasting

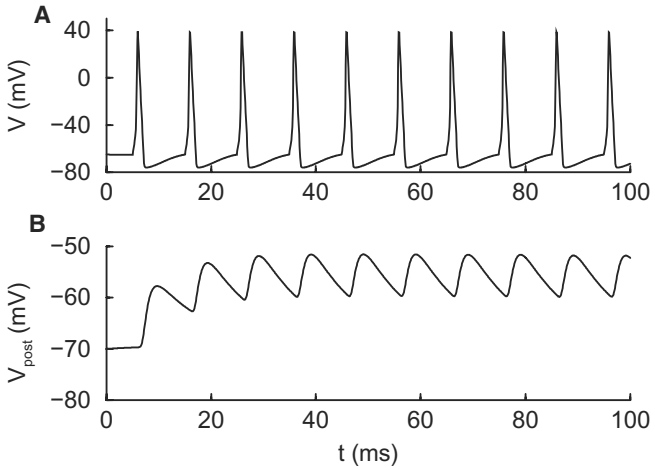

Fig. 6. Simulated postsynaptic response to a presynaptic train of impulses. The postsynaptic membrane time constant and the stimulus frequency determine the degree of summation in the postsynaptic response

9 Short-Term Plasticity

The synapse is highly plastic, exhibiting several forms of short-term and long-term plasticity. Long-term plasticity occurs in both presynaptic and postsynaptic regions and typically involves insertion of receptors or channels into the membrane and/or targeted gene expression. Short-term plasticity is often accomplished without any structural modifications to the synapse, and can be due to things such as Ca^{2+} accumulation, activation of second messengers, and phosphorylation (Zucker and Regehr, 2002). Our focus will be on short-term plasticity.

Short-term plasticity is often measured using a paired-pulse protocol. Here, the presynaptic neuron is stimulated twice, with an interstimulus interval of δt. The postsynaptic response, either current or potential, is recorded for each stimulus, and the ratio of the second response to the first is the measure of plasticity, $SP_2 = P_2/P_1$. If $SP_2 > 1$ then the second response is facilitated; if $SP_2 < 1$ then the second response is depressed. The duration of the facilitation or depression is determined by increasing δt until $SP_2 \approx 1$.

Another protocol used to measure plasticity is to apply an impulse train (often called a "tetanus") to the presynaptic neuron and record the postsynaptic response throughout the train. Then $SP_n = P_n/P_1$ provides a measure of the enhancement or depression of the nth response relative to the first. It is not uncommon for SP_n to indicate enhancement at the beginning of the train and depression later in the train, as various plasticity mechanisms compete with different time scales. A variation of this stimulus protocol is to induce a "conditioning" impulse train and then, at a time δt following the train, to

induce a single impulse, the "test stimulus". The ratio of the postsynaptic responses to the test stimulus with and without the conditioning train then provides a measure of plasticity induced by the train. Often δt is varied to determine the time constant of decay of the plasticity.

Synaptic enhancement occurs at several time scales. **Facilitation** occurs at the fastest time scale, and is often measured using a paired-pulse protocol (Fig. 13). This type of enhancement is often subdivided into F1 facilitation, which lasts tens of milliseconds, and F2 facilitation, which lasts hundreds of milliseconds. **Augmentation** develops during an impulse train, and grows and decays with a time constant of 5–10 sec. Finally, **post-tetanic potentiation** is like augmentation in that it is induced by an impulse train, however it is longer-lasting, with a time constant of ≈ 30 sec. The distinct time constants for the various forms of enhancement suggest that they are produced by different mechanisms.

Synaptic **depression** is observed in most central nervous system synapses and less frequently in neuromuscular junctions. In central synapses, the postsynaptic response typically declines throughout a train of presynaptic stimuli (Fig. 7), or first rises and then declines later in the train. In many cases the degree of depression increases with the stimulus frequency (Abbott et al., 1997; Tsodyks and Markram, 1997), although in some cases the opposite is true (Shen and Horn, 1996). This difference in the frequency dependence of depression suggests at least two mechanisms for this form of plasticity.

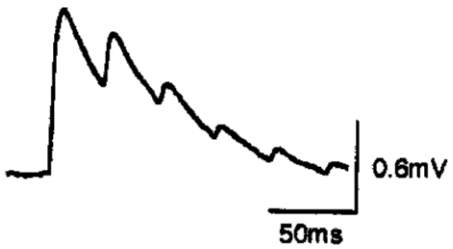

Fig. 7. The postsynaptic response depresses throughout a train of presynaptic impulses in this pyramidal neuron from the rat cortex. Reprinted with permission from Markram et al. (1998a)

10 Mathematical Models for Facilitation

The mechanism for facilitation of transmitter release has been debated for more than three decades, ever since Katz and Miledi (1968) and Rahamimoff (1968) suggested that facilitation is due to the buildup of Ca^{2+} bound to release sites. It has been clear from the beginning that Ca^{2+} plays a key role, but the difficulties inherent in measuring Ca^{2+} microdomains, and the

small size of the synapse, has obscured the mechanism by which Ca^{2+} produces facilitation. Thus, mathematical models of various facilitation mechanisms have been developed, and predictions from these models compared with experiments. Three main mechanisms for facilitation have been postulated: (1) residual free Ca^{2+}, (2) residual bound Ca^{2+}, and (3) saturation of endogenous Ca^{2+} buffers. Models for each of these will be discussed below, beginning with a series of models developed by Zucker and colleagues for a residual free Ca^{2+} mechanism of facilitation.

11 Residual Free Ca^{2+} Models

The Fogelson-Zucker model (Fogelson and Zucker, 1985) was developed to describe transmitter release and its facilitation in the squid giant synapse. The authors first considered a model in which Ca^{2+} diffuses in one dimension. Cylindrical coordinates were used, and it was assumed that Ca^{2+} enters through the whole surface membrane of the terminal and diffuses only in the radial direction. The model included stationary buffers. The authors also considered a 3-dimensional Ca^{2+} diffusion model where Ca^{2+} enters through an array of channels in the terminal membrane. Each channel was considered to be a point source on the boundary. Transmitter release was modeled as a power of the free Ca^{2+} concentration in the terminal, $R = kCa_{bk}^n$. The stoichiometry $n = 5$ was chosen to best fit experimental data on facilitation in the squid synapse.

The main result of this work was that during a train of impulses the free Ca^{2+} concentration in the terminal could accumulate, and could potentially account for the facilitation in transmitter release observed in the squid synapse. That is, since $R = kCa_{bk}^5$ and since Ca_{bk} builds up during the impulse train, the release from each impulse is facilitated relative to that from the previous impulse. Importantly, this model predicts that it is the diffusion of Ca^{2+} that determines both transmitter release and its facilitation, and that other factors such as the kinetics of Ca^{2+} binding to or unbinding from the release sites, or the effects of mobile buffers, are secondary.

The Fogelson-Zucker model motivated many experimental studies aimed at testing this residual free Ca^{2+} mechanism for facilitation. Parnas and colleagues pointed out that the Fogelson-Zucker model failed to account for several experimental findings (Parnas et al., 1989). In particular, facilitation has been shown to be very dependent on temperature, while the diffusion of Ca^{2+} would only be weakly temperature dependent. They also pointed to some early experiments by Datyner and Gage, who studied the shape of the release time course during facilitation and with different concentrations of external Ca^{2+} by normalizing the peaks of the responses (Datyner and Gage, 1980). Inducing a train of three presynaptic impulses at 65 Hz, they found that although the response clearly facilitated, the normalized time course was invariant throughout the train (Fig. 8). Similarly, they found time course invariance

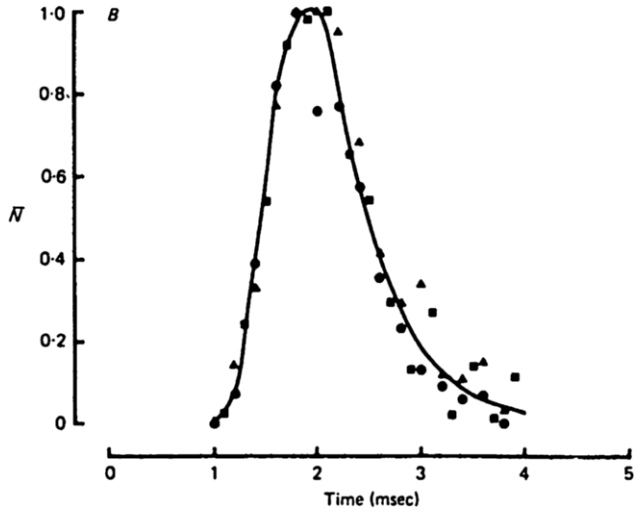

Fig. 8. The normalized release time course is invariant during a 65 Hz train of three stimuli that produces facilitation. Responses to the first (*circles*), second (*triangles*), and third stimulus (*squares*) normalized to have the same peak values. Reprinted with permission from Datyner and Gage (1980)

when comparing the response in low external Ca^{2+} and high external Ca^{2+} (the latter produced a larger peak response). Parnas and colleagues pointed out that the Fogelson-Zucker model did not exhibit time course invariance. A final criticism of the model was that the colocalization of low-affinity Ca^{2+} acceptors and Ca^{2+} channels makes it unlikely that a small (sub-micromolar) buildup in the Ca^{2+} concentration could have a significant effect on the magnitude of Ca^{2+} release.

A second-generation residual free Ca^{2+} model that addressed these problems was developed by Yamada and Zucker (1992). As in the earlier model, intraterminal Ca^{2+} diffused in three dimensions. Now, however, the Ca^{2+} binding kinetics at Ca^{2+} acceptors on the release sites were included. The authors assumed that there are four identical low-affinity acceptors (denoted by X) that act as triggers to secretion, and a high-affinity site (denoted by Y) that is responsible for facilitation. The kinetic relations are:

$$X + Ca \underset{k_x^-}{\overset{4k_x^+}{\rightleftarrows}} CaX + Ca \underset{2k_x^-}{\overset{3k_x^+}{\rightleftarrows}} Ca_2X + Ca \underset{3k_x^-}{\overset{2k_x^+}{\rightleftarrows}} Ca_3X + Ca \underset{4k_x^-}{\overset{k_x^+}{\rightleftarrows}} Ca_4X$$

and

$$Y + Ca \underset{k_y^-}{\overset{k_y^+}{\rightleftarrows}} CaY.$$

Release occurs when all four X sites are bound and the Y site is bound,

$$Ca_4X + CaY \underset{k_r^-}{\overset{k_r^+}{\rightleftharpoons}} R$$

The binding kinetics are converted to differential equations using the law of mass action.

As in the Fogelson-Zucker model, most of the facilitation in this model is due to the buildup of free Ca^{2+}. During a train of impulses Ca^{2+} accumulates and binds to the high-affinity Y sites, which bind and unbind Ca^{2+} slowly. These slow rates average the fast Ca^{2+} signals generated by impulses during an impulse train, and make this a hybrid residual free Ca^{2+}/residual bound Ca^{2+} model. The temperature dependence of facilitation is easily explained as a temperature-dependent effect on Ca^{2+} binding to the Y site. In addition, the normalized release time course is relatively invariant during a facilitating train and when the external Ca^{2+} concentration is changed.

Following publication of the Yamada-Zucker model a key experiment was performed showing that facilitation, augmentation, and post-tetanic potentiation were all reduced following activation of the photolabile Ca^{2+} chelator diazo-2 (Kamiya and Zucker, 1994). This chelator has low Ca^{2+} affinity unless photolyzed by UV light, which greatly increases the affinity. Diazo-2 was injected iontophoretically into an isolated crayfish motor neuron. Following injection, a train of presynaptic impulses was induced and the end junction potential (e.j.p.) recorded. The response was clearly facilitated by the end of the 10-impulse train. This facilitation was reduced by half (but not eliminated) when a UV light flash was applied prior to the test impulse at the end of the train (Fig. 9). Since UV light increases the Ca^{2+} affinity of diazo-2 to a value similar to that of BAPTA, the natural conclusion was that the photoactivated diazo-2 buffered down the residual free Ca^{2+} and thereby reduced the facilitation. Additional experiments using the Ca^{2+} chelators BAPTA and EGTA generally support the hypothesis that residual free Ca^{2+} is a key element of facilitation and other forms of short-term enhancement (Atluri and Regehr, 1996; Fischer et al., 1997a). It should be noted, however, that some labs have found that Ca^{2+} chelators have no effect on facilitation (Robitaille and Charlton, 1991; Winslow et al., 1994).

The rapid rate at which facilitation was reduced by activated diazo-2 was at odds with the slow-unbinding facilitation site postulated by Yamada and Zucker. However, if the unbinding rate were increased to satisfy the Kamiya-Zucker experiment, then the dynamics of the Y site would be determined more by the opening and closing of the colocalized channel than by the residual free Ca^{2+}. For this reason, the Zucker group formulated a new model of transmitter release and facilitation in which the high-affinity facilitation site is located away from a Ca^{2+} channel (Tang et al., 2000). In this model, three low-affinity X sites are postulated, at a distance of 10–20 nm from a Ca^{2+} channel. The high-affinity Y site is postulated to lie 80–100 nm from the nearest Ca^{2+} channel. The kinetics are basically the same as in the Yamada-Zucker model,

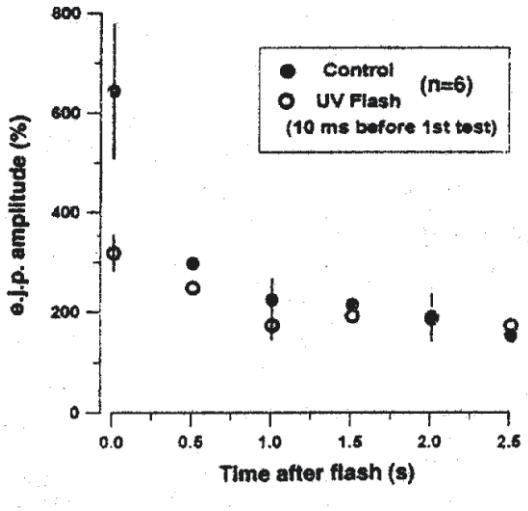

Fig. 9. Facilitation following a 50 Hz train of 10 impulses was reduced following UV activation of the photolabile Ca^{2+} chelator diazo-2. Data from a crayfish motor neuron. Reprinted with permission from Kamiya and Zucker (1994)

except that the Y site is now assumed to unbind Ca^{2+} rapidly, allowing the model to reproduce the Kamiya-Zucker experiment.

The Tang et al. model also aimed to reproduce the authors' experiments showing that both the accumulation and the decay of facilitation are affected by the fast high-affinity Ca^{2+} buffer fura-2 and that facilitation grows supralinearly during an impulse train (Tang et al., 2000). Unfortunately, the computer software developed for the model had several errors, and although the model originally seemed to reproduce most of the data, once the errors were corrected the fit to the data was not good (Matveev et al., 2002). However, once the corrected model was recalibrated, it was able to reproduce most of the data, but not all, from Tang et al. Significantly, the model was able to produce supralinear faciliation, and the facilitation was reduced when a high-affinity buffer was simulated (Fig. 10). The success of the model simulations required several stringent assumptions. It was necessary to assume that the high-affinity buffer fura-2 is immobilized and the Ca^{2+} diffusion coefficient is reduced fivefold near the active zone, possibly due to tortuosity. It was also necessary to reduce the diffusion coefficient of fura-2 100-fold in the rest of the terminal (Matveev et al., 2002). Since these assumptions are questionable, it would seem that while this latest implementation of the residual free Ca^{2+} hypothesis captures some features of facilitation, significant modifications are needed to fully explain the phenomenon.

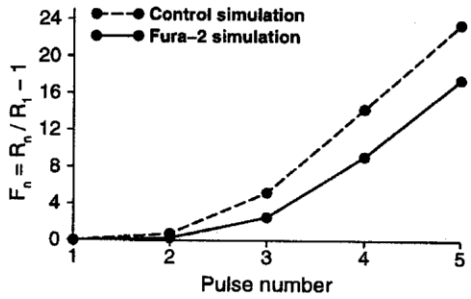

Fig. 10. In the model of Matveev et al. (2002), faciliation grows supralinearly during a pulse train. The degree of facilitation is reduced by simulated application of the high-affinity buffer fura-2. Reprinted with permission from Matveev et al. (2002)

12 A Residual Bound Ca^{2+} Model for Facilitation

The mechanism originally proposed by Katz and Miledi (1968) and Rahamimoff (1968), that facilitation is due to the accumulation of Ca^{2+} bound to release sites, fell out of favor as models for a residual free Ca^{2+} mechanism established the dominant paradigm. This paradigm was challenged by an alternate hypothesis of Stanley (Stanley, 1986) that was implemented as a mathematical model by Bertram et al. (1996). This was based on experimental data from the squid giant synapse suggesting that the Ca^{2+} cooperativity of transmitter release decreased during facilitation, and that the steady-state facilitation increased in a step-like fashion with the stimulus frequency (Stanley, 1986). Bertram et al. showed that both of these phenomena could be explained if one assumed that each release site has four Ca^{2+} acceptors with differing Ca^{2+} affinities and unbinding rates.

In this model, each Ca^{2+} acceptor can be described by a first order kinetic scheme,

$$U_j + Ca \underset{k_j^-}{\overset{k_j^+}{\rightleftarrows}} B_j$$

where U_j represents an unbound acceptor ($j = 1{-}4$, for the four acceptors) and B_j represents a Ca^{2+}-bound acceptor. Release occurs when all four acceptors are occupied,

$$R = B_1 B_2 B_3 B_4 \,. \tag{20}$$

Binding and unbinding rates, k_j^+ and k_j^- respectively, were chosen to produce steps in the frequency-dependence of facilitation. These gave unbinding time constants ($1/k_j^-$) of 2.5 s, 1 s, 10 ms, and 0.1 ms, and dissociation constants (k_j^-/k_j^+) of 108 nM, 400 nM, 200 µM, and 1,334 µM for the four acceptors (denoted S_1–S_4).

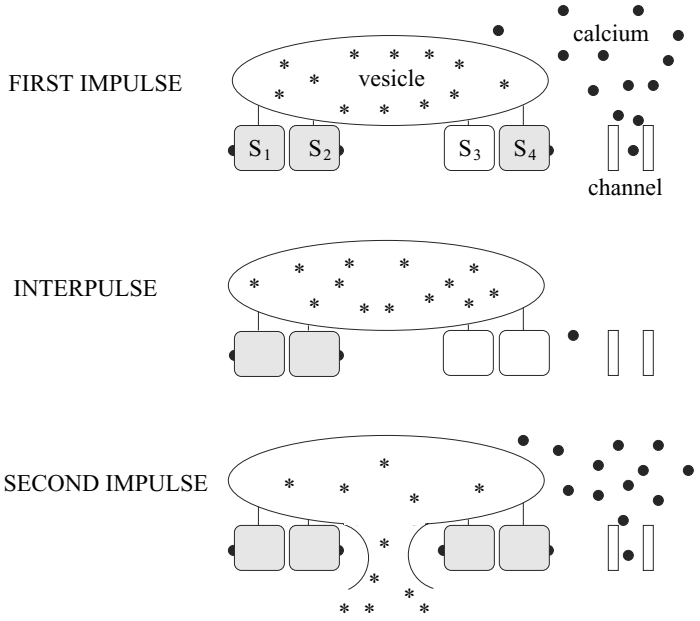

Fig. 11. Illustration of the residual bound Ca^{2+} model of facilitation by Bertram et al. (1996). Each box represents a Ca^{2+} acceptor. Reprinted from Bertram and Sherman (1998)

The mechanism by which step-like facilitation is produced with this model is illustrated in Fig. 11. Prior to the first presynaptic impulse none of the acceptors are occupied. With the first impulse, a colocalized Ca^{2+} channel opens, and Ca^{2+} entering through the channel forms a microdomain. In this illustration, Ca^{2+} within the microdomain binds to three of the four acceptors. Since one acceptor remains unbound the vesicle does not fuse with the membrane. After the first impulse Ca^{2+} unbinds from the acceptor with the smallest unbinding time constant (site S_4). However, if the second impulse arrives before Ca^{2+} can unbind from sites S_1 and S_2 then Ca^{2+} from this second impulse must only bind to two of the four acceptors to induce vesicle fusion and transmitter release. In this way, using a residual bound Ca^{2+} mechanism, the release probability is facilitated. The reduced number of sites needed to gate facilitated release accounts for the drop in the Ca^{2+} cooperativity reported by Stanley, and the three distinct slow unbinding rates account for the three steps in the frequency-dependence of facilitation. Because facilitation in this model is due to slow Ca^{2+} unbinding rather than buildup of free Ca^{2+}, the mechanism would be highly temperature dependent. Also, simulations and mathematical analysis showed that the release time course exhibits the required invariance properties (Bertram et al., 1996; Bertram and Sherman, 1998). However, this model does not account for the reduction of facilitation

caused by Ca^{2+} chelators. In particular, it does not reproduce the results of the Kamiya-Zucker diazo-2 experiment, unless modified to include effects of residual free Ca^{2+} as well as residual bound Ca^{2+}.

13 A Model for Facilitation Based on Buffer Saturation

Another mechanism for facilitation was suggested by simulations of Ca^{2+} and buffer diffusion near a membrane (Klingauf and Neher, 1997; Neher, 1998). In this model, Ca^{2+} buffer saturates during an impulse train, so that the amount of free Ca^{2+} introduced near the membrane by an impulse increases throughout the train, producing facilitated transmitter release.

The conditions in which buffer can saturate and produce facilitation were clarified in a study by Matveev et al. (2004). They found that robust facilitation can be achieved either by a global saturation of a highly mobile buffer (like fura-2 or BAPTA) in the entire presynaptic terminal, or saturation of an immobile buffer local to the release sites. Figure 12 shows how facilitation occurs with this mechanism. Here a 100 Hz train of equal Ca^{2+} current pulses is applied to the model terminal. A mobile buffer is present at a concentration of 500 µM (free buffer concentration is plotted in the bottom panel). The free Ca^{2+} concentration a distance of 60 nM from a cluster of channels is shown in the middle panel. During the first pulse Ca^{2+} concentration rises and binds

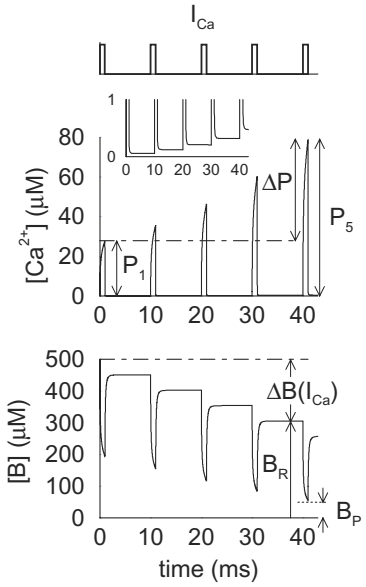

Fig. 12. In this simulation by Matveev et al. (2004) the free Ca^{2+} concentration rises to a higher level with each successive pulse of Ca^{2+} current, due to the saturation of mobile buffer. Reprinted with permission from Matveev et al. (2004)

to buffer, transiently reducing the free buffer concentration. Between the first and second pulse much of the Ca^{2+} is extruded from the terminal, but some remains in equilibrium with the buffer. This residual binding to buffer decreases the amount of buffer available to chelate Ca^{2+} during the second pulse, so the free Ca^{2+} concentration rises to a higher level during the second pulse (middle panel), resulting in facilitated transmitter release.

There is recent experimental evidence supporting the buffer saturation mechanism for facilitation. Blatow et al. (2003) examined terminals of GABAergic interneurons in the mouse neocortex and mouse hippocampal mossy fiber terminals. Both of these contain the endogenous fast Ca^{2+} buffer calbindin-D28k (CB), and facilitation is robust. In the interneuron synapses, CB knockout eliminated the facilitation. However, facilitation was rescued by addition of the exogenous buffer BAPTA. That is, in these terminals addition of a high-affinity buffer increased facilitation, contrary to what would be expected if facilitation were due to either residual free or bound Ca^{2+}. Another property of the buffer saturation mechanism is that facilitation should increase when the external Ca^{2+} concentration is raised, since the resulting greater Ca^{2+} influx would produce more buffer saturation. In other models of facilitation this maneuver would decrease facilitation (Zucker, 1989). Blatow et al. showed that in the CB-containing mossy fiber terminals the facilitation increased when external Ca^{2+} concentration was raised (Fig. 13). Interestingly, they also showed that a second type of excitatory synapse in the hippocampus, the Schaffer collateral to CA1 pyramidal cell synapse, has properties consistent with a residual free Ca^{2+} mechanism for facilitation. Further, in CB knockouts in mossy fiber synapses, facilitation was reduced but not lost. The residual facilitation had all the properties expected from a residual free Ca^{2+} mechanism (Fig. 13).

The study by Blatow et al. (2003) not only provides strong evidence for the buffer saturation mechanism for facilitation, but it also serves as an excellent demonstration that different facilitation mechanisms may exist in different synapses, and that facilitation in some synapses may be due to a combination of mechanisms.

14 Synaptic Depression

Use-dependent depression of transmitter release is common in central synapses. This is reflected in a reduction in the magnitude of the postsynaptic current elicited by action potentials in an impulse train (Fig. 7). One mechanism for this is the partial depletion of the readily releasable pool of vesicles (Zucker and Regehr, 2002). Simply put, prior impulses reduce the number of primed vesicles that can be released by subsequent impulses. The recovery time from this form of depression is determined by the time required to refill the readily releasable pool.

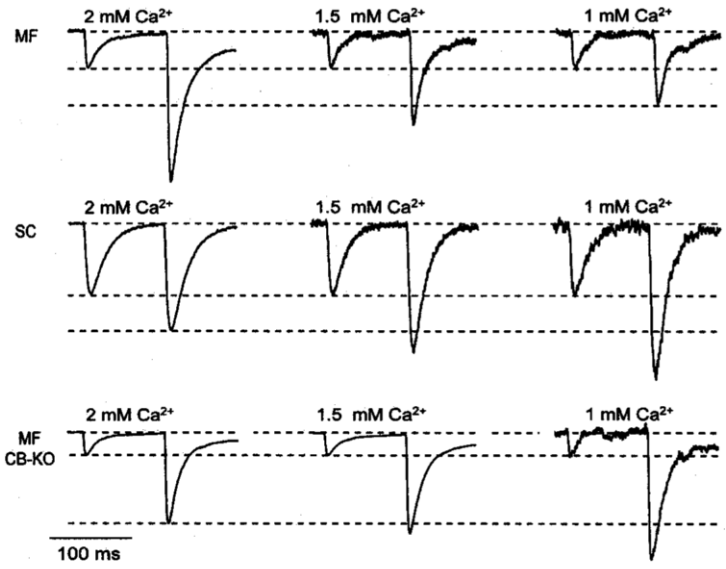

Fig. 13. In mossy fiber (MF) terminals containing CB, paired pulse facilitation becomes larger as the external Ca^{2+} concentration is increased. In Schaffer collateral (SC) synapses, facilitation decreases. In MF terminals with CB knocked out, the effect of external Ca^{2+} on facilitation is the same as in SC terminals. Reprinted with permission from Blatow et al. (2003)

An interesting link between depression and information processing was made by Abbott et al. (1997) and Tsodyks and Markram (1997). Cortical and neocortical neurons receive synaptic input from thousands of afferents, which fire at rates ranging from a few Hz to several hundred Hz. If synapses responded linearly to the presynaptic impulse frequency, then high-frequency inputs would dominate low-frequency inputs. Depression prevents this from happening by acting as a gain control, reducing the responses to impulses in high-frequency trains proportionally to the frequency of the train. That is, if $A(r)$ denotes the steady state postsynaptic response amplitude to an impulse in a train of frequency r, then for r sufficiently large $A(r) \propto 1/r$ in cortical and neocortical synapses. Thus, the total synaptic conductance during one second of stimulation, $rA(r)$, is approximately constant at all frequencies above some threshold (Fig. 14). In this way, low- and high- frequency trains are equalized.

Suppose that an impulse train is applied at frequency r and the system reaches a steady state. Now suppose that the frequency is suddenly changed by Δr. Before the system has established its new steady state, the change in the synaptic response (ΔR) is

$$\Delta R = \Delta r A(r) \approx \Delta r / r \; . \tag{21}$$

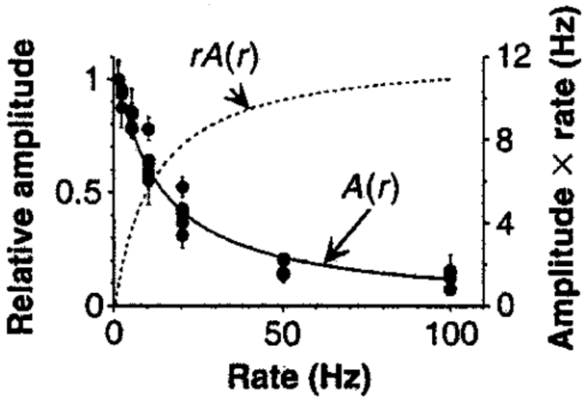

Fig. 14. In synapses of cortical neurons, the steady state postsynaptic response amplitude $A(r)$ has a $1/r$ dependence on the stimulus frequency r. The total synaptic response per second of stimulus, $rA(r)$, is roughly constant above a threshold frequency. Reprinted with permission from Abbott et al. (1997)

Thus, an increase from 10 Hz to 11 Hz ($\Delta r/r = 0.1$) will have the same initial effect as an increase from 100 Hz to 110 Hz ($\Delta r/r = 0.1$). That is, the change in the initial response is proportional to the **relative change** in the input frequency (Abbott et al., 1997; Tsodyks and Markram, 1997). The ability of neurons to sense relative changes in stimuli is a highly desirable feature, and it is remarkable that a mechanism for this is something as simple as depletion of resources.

15 G Protein Inhibition of Presynaptic Ca^{2+} Channels

Depletion of the readily releasable vesicle pool is not the only mechanism for synaptic depression. Another common mechanism is through the action of G proteins. The presynaptic terminal contains various G protein-coupled receptors. These receptors are activated by a variety of ligands, including the neurotransmitters GABA, adenosine, glutamate, dopamine and serotonin (Hille, 1994). Binding of a ligand molecule to a receptor activates the associated G protein. The G protein is a heterotrimer, with α, β, and γ subunits. When activated, GTP replaces GDP bound to the G protein, and the Gα subunit dissociates from the G$\beta\gamma$ dimer, which remains tethered to the membrane. Once activated in this way, G$\beta\gamma$ can bind to Ca^{2+} channels, putting them into a **reluctant state**, with a decreased opening rate and an increased closing rate (Ikeda, 1996).

The agonist for the G protein-coupled receptor can be a hormone, or it can be released from the postsynaptic neuron, or from the presynaptic terminal itself (Fig. 15). In fact, many synapses have G protein-coupled autoreceptors that are specific for the transmitter released from the terminal (Wu and

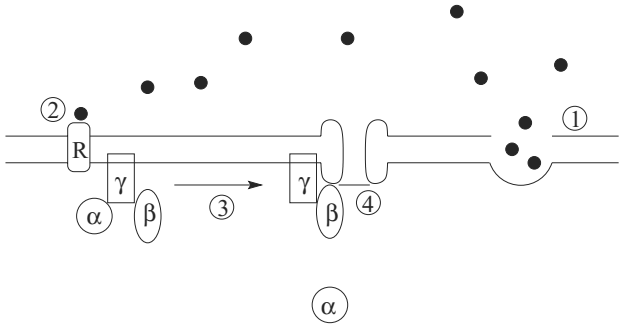

Fig. 15. Transmitter released from the presynaptic terminal (1) can bind to a G protein-coupled autoreceptor (2), activating the associated G protein (3). The G$\beta\gamma$ dimer can then bind to a Ca^{2+} channel (4), putting it into a reluctant state

Saggau, 1997; Chen and van den Pol, 1998) and G protein-mediated autoinhibition has been demonstrated under physiological conditions (Benoit-Marand et al., 2001).

An interesting feature of G protein inhibition of Ca^{2+} channels is that in most cases the inhibition is relieved by membrane depolarization. This is due to the unbinding of G$\beta\gamma$ from the Ca^{2+} channel (Zamponi and Snutch, 1998). Thus, depolarization of the terminal has two opposing effects. One is to elicit transmitter release, which results in activation of G proteins through autoreceptor binding. The increased G protein activation tends to inhibit further transmitter release. The second effect of depolarization is to cause activated G proteins to unbind from the Ca^{2+} channels, relieving the inhibition. Thus, the overall effect of the G protein pathway will depend upon which of these two opposing actions dominates.

A mathematical model for the action of G proteins on Ca^{2+} channels was developed by Boland and Bean (1993). This model was subsequently simplified and coupled to a model of transmitter release and autoreceptor binding (Bertram and Behan, 1999). Through numerical simulations, it was shown that G protein autoinhibition acts as a high-pass filter, allowing high-frequency trains of impulses to pass from the presynaptic to the postsynaptic cell, while low-frequency trains are filtered out (Bertram, 2001). The high-frequency trains are transmitted since the mean membrane potential of the synapse is elevated during such trains, relieving the G protein inhibition. Low-frequency trains result in less transmitter release, and thus a lower level of G protein activation, but those G proteins that are activated are much more effective at inhibiting Ca^{2+} channels and subsequent transmitter release.

One role of the G protein-induced high-pass filtering could be to remove noise, in the form of low-frequency signals, from a neural system. For example, consider a neural network in which a 5-by-5 input layer of neurons innervates a 5-by-5 output layer. Suppose that the G protein pathway operates in each of the input layer synapses. Finally, suppose that a signal in the input layer

is degraded by low-frequency noise (Fig. 16A). Here, the signal is a spatial pattern (an X) consisting of high-frequency impulse trains in 5 of the input layer neurons. Other input-layer neurons produce impulse trains at various lower frequencies (color and size coded in Fig. 16). Because of the filtering action of G proteins, the signal is transmitted to the postsynaptic cells, while the noise is attenuated (Fig. 16B). Thus, the G protein pathway effectively increases the spatial contrast of the "image".

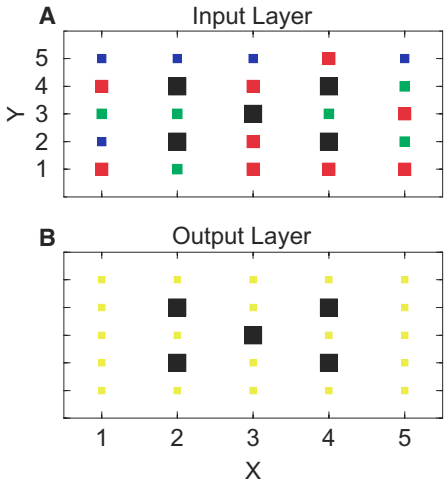

Fig. 16. G protein-mediated high-pass filtering can increase the spatial contrast of an image by increasing the signal-to-noise ratio. **(A)** A 5×5 grid of input cells fires at various frequencies r (Black, $r > 100$ Hz; red, $70 < r \leq 100$; green, $40 < r \leq 70$; blue, $10 < r \leq 40$; yellow, $r < 10$). **(B)** Each cell in the 5×5 output layer recieves synaptic input from one cell in the input layer. As a result of autoinhibition of the presynaptic transmitter release, the signal-to-noise ratio in the output layer is much greater than that in the input layer. Reprinted from Bertram et al. (2002)

16 Conclusion

Mathematical modeling and computer simulations have played a large role in unveiling the mechanisms of synaptic transmitter release and its short term plasticity. Yet, while progress has been made, there is much that remains unclear. For example, none of the models of facilitation can account for all of the key features of the experimental data from the crayfish neuromuscular junction. How should these models be modified or combined to better account for the data? What is the best way to model Ca^{2+} in the terminal? Solving 3-dimensional reaction diffusion equations is the most accurate method, but is

the simpler approach of using steady state approximations sufficient in many cases? The answer to this will certainly depend on the extend of overlap of Ca^{2+} microdomains at the release sites, which may vary greatly from synapse to synapse. It appears that there is still a great deal of modeling and analysis of transmitter release and its plasticity that can be done, in parallel with the many experimental studies that are being performed with ever-improving tools.

Acknowledgements

The author thanks the National Science Foundation for financial support through grant DMS-0311856.

References

L. F. Abbott, J. A. Varela, K. Sen, and S. B. Nelson, *Synaptic depression and cortical gain control*, Science, 275 (1997), pp. 220–224. 185, 194, 195

S. Aharon, H. Parnas, and I. Parnas, *The magnitude and significance of Ca^{2+} domains for release of neurotransmitter*, Bull. Math. Biol., 56 (1994), pp. 1095–1119. 173

N. L. Allbritton, T. Meyer, and L. Stryer, *Range of messenger action of calcium ion and inositol 1,4,5-trisphophate*, Science, 258 (1992), pp. 1812–1815. 176

P. P. Atluri and W. G. Regehr, *Determinants of the time course of facilitation at the granule cell to Purkinje cell synapse*, J. Neurosci., 16 (1996), pp. 5661–5671. 188

G. J. Augustine, M. P. Charlton, and S. J. Smith, *Calcium entry and transmitter release at voltage-clamped nerve terminals of squid*, J. Physiol. (Lond.), 367 (1985), pp. 163–181. 177

M. Benoit-Marand, E. Borrelli, and F. Gonon, *Inhibition of dopamine release via presynaptic D2 receptors: Time course and functional characteristics* in vivo, J. Neurosci., 21 (2001), pp. 9134–9141. 196

R. Bertram, *A simple model of transmitter release and facilitation*, Neural Comput., 9 (1997), pp. 515–523. 182

———, *Differential filtering of two presynaptic depression mechanisms*, Neural Comput., 13 (2001), pp. 69–85. 196

R. Bertram, M. I. Arnot, and G. W. Zamponi, *Role for G protein $G\beta\gamma$ isoform specificity in synaptic signal processing: A computational study*, J. Neurophysiol., 87 (2002), pp. 2612–2623. 197

R. Bertram and M. Behan, *Implications of G-protein-mediated Ca^{2+} channel inhibition for neurotransmitter release and facilitation*, J. Comput. Neurosci., 7 (1999), pp. 197–211. 196

R. Bertram and A. Sherman, *Population dynamics of synaptic release sites*, SIAM J. Appl. Math., 58 (1998), pp. 142–169. 173, 182

R. Bertram, A. Sherman, and E. F. Stanley, *Single-domain/bound calcium hypothesis of transmitter release and facilitation*, J. Neurophysiol., 75 (1996), pp. 1919–1931. 173, 174, 190

R. Bertram, G. D. Smith, and A. Sherman, *A modeling study of the effects of overlapping Ca^{2+} microdomains on neurotransmitter release*, Biophys. J., 76 (1999), pp. 735–750. 173, 180

M. Blatow, A. Caputi, N. Burnashev, H. Monyer, and A. Rozov, *Ca^{2+} buffer saturation underlies paired pulse facilitation in calbindin-D28k-containing terminals*, Neuron, 38 (2003), pp. 79–88. 193

L. M. Boland and B. P. Bean, *Modulation of N-type calcium channels in bullfrog sympathetic neurons by luteinizing hormone-releasing hormone: kinetics and voltage dependence*, J. Neurosci., 13 (1993), pp. 516–533. 196

G. Chen and A. N. van den Pol, *Presynaptic $GABA_B$ autoreceptor modulation of P/Q-type calcium channels and GABA release in rat suprachiasmatic nucleus neurons*, J. Neurosci., 18 (1998), pp. 1913–1922. 196

N. B. Datyner and P. W. Gage, *Phasic secretion of acetylcholine at a mammalian neuromuscular junction*, J. Physiol. (Lond.), 303 (1980), pp. 299–314. 186

A. Destexhe, Z. F. Mainen, and T. J. Sejnowski, *Synthesis of models for excitable membranes, synaptic transmission and neuromodulation using a common kinetic formalism*, J. Comput. Neurosci., 1 (1994), pp. 195–230. 180, 181

F. A. Dodge, Jr. and R. Rahamimoff, *Co-operative action of calcium ions in transmitter release at the neuromuscular junction*, J. Physiol. Lond, 193 (1967), pp. 419–432. 174

T. M. Fischer, R. S. Zucker, and T. J. Carew, *Activity-dependent potentiation of synaptic transmission from L30 inhibitory interneurons of* aplysia *depends on residual presynaptic Ca^{2+} but not on postsynaptic Ca^{2+}*, J. Neurophysiol., 78 (1997), pp. 2061–2071. 188

A. L. Fogelson and R. S. Zucker, *Presynaptic calcium diffusion from various arrays of single channels*, Biophys. J., 48 (1985), pp. 1003–1017. 173, 175, 186

M. Geppert, Y. Goda, R. E. Hammer, C. Li, T. W. Rosahl, C. F. Stevens, and T. C. Südhof, *Synaptotagmin I: A major Ca^{2+} sensor for transmitter release at a central synapse*, Cell, 79 (1994), pp. 717–727. 174

Y. Goda, *SNAREs and regulated vesicle exocytosis*, Proc. Natl. Acad. Sci. USA, 94 (1997), pp. 769–772. 174

R. Heidelberger, C. Heinemann, E. Neher, and G. Matthews, *Calcium dependence of the rate of exocytosis in a synaptic terminal*, Nature, 371 (1994), pp. 513–515. 173, 175

B. Hille, *Modulation of ion-channel function by G-protein-coupled receptors*, Trends Neurosci., 17 (1994), pp. 531–536. 195

B. Hochner, H. Parnas, and I. Parnas, *Membrane depolarization evokes neurotransmitter release in the absence of calcium entry*, Nature, 342 (1989), pp. 433–435. 173

S. R. Ikeda, *Voltage-dependent modulation of N-type calcium channels by G-protein $\beta\gamma$ subunits*, Nature, 380 (1996), pp. 255–258. 195

S. E. Jarvis, W. Barr, Z. P. Feng, J. Hamid, and G. W. Zamponi, *Molecular determinants of syntaxin 1 modulation of N-type calcium channels*, J. Biol. Chem., 277 (2002), pp. 44399–44407. 175

H. Kamiya and R. S. Zucker, *Residual Ca^{2+} and short-term synaptic plasticity*, Nature, 371 (1994), pp. 603–606. 173, 188

B. Katz and R. Miledi, *The role of calcium in neuromuscular facilitation*, J. Physiol. (Lond.), 195 (1968), pp. 481–492. 185

J. Klingauf and E. Neher, *Modeling buffered Ca^{2+} diffusion near the membrane: Implications for secretion in neuroendocrine cells*, Biophys. J., 72 (1997), pp. 674–690. 173, 175, 176, 192

R. Llinás, I. Z. Steinberg, and K. Walton, *Presynaptic calcium currents and their relation to synaptic transmission: Voltage clamp study in squid giant synapse and theoretical model for the calcium gate*, Proc. Natl. Acad. Sci. USA, 73 (1976), pp. 2918–2922. 175

H. Markram, Y. Wang, and M. Tsodyks, *Differential signaling via the same axon of neocortical pyramidal neurons*, Proc. Natl. Acad. Sci. USA, 95 (1998), pp. 5323–5328. 185

V. Matveev, A. Sherman, and R. S. Zucker, *New and corrected simulations of synaptic function*, Biophys. J., 83 (2002), pp. 1368–1373. 173, 175, 189

V. Matveev, R. S. Zucker, and A. Sherman, *Facilitation through buffer saturation: constraints on endogenous buffering properties*, Biophys. J., 86 (2004), pp. 2691–2709. 175, 192

M. Naraghi and E. Neher, *Linearized buffered Ca^{2+} diffusion in microdomains and its implications for calculation of $[Ca^{2+}]$ at the mouth of a calcium channel*, J. Neurosci., 17 (1997), pp. 6961–6973. 48, 173, 175

E. Neher, *Concentration profiles of intracellular calcium in the presence of a diffusible chelator*, in Calcium Electrogenesis and Neuronal Functioning, U. Heinemann, M. Klee, E. Neher, and W. Singer, eds., Springer-Verlag, Berlin, 1986, pp. 80–96. 175, 178

———, *Usefulness and limitations of linear approximations to the understanding of Ca^{2+} signals*, Cell Calcium, 24 (1998), pp. 345–357. 192

H. Parnas, G. Hovav, and I. Parnas, *Effect of Ca^{2+} diffusion on the time course of neurotransmitter release*, Biophys. J., 55 (1989), pp. 859–874. 186

H. Parnas and L. A. Segel, *A theoretical study of calcium entry in nerve terminals, with application to neurotransmitter release*, J. theor. Biol., 91 (1981), pp. 125–169. 173

R. Pethig, M. Kuhn, E. Payne, T. Chen, and L. F. Jaffe, *On the dissociation constants of BAPTA-type Ca^{2+} buffers*, Cell Calcium, 10 (1989), pp. 491–498. 176

R. Rahamimoff, *A dual effect of calcium ions on neuromuscular facilitation*, J. Physiol. (Lond.), 195 (1968), pp. 471–480. 185

W. Rall, *Distinguishing theoretical synaptic potentials computed for different soma-dendritic distributions of synaptic inputs*, J. Neurophysiol., 30 (1967), pp. 1138–1168. 181

R. Rao-Mirotznik, A. B. Harkins, G. Buchsbaum, and P. Sterling, *Mammalian rod terminal: architecture of a binary synapse*, Neuron, 14 (1995), pp. 561–569. 175

J. Rettig and E. Neher, *Emerging roles of presynaptic proteins in Ca^{2+}-triggered exocytosis*, Science, 298 (2002), pp. 781–785. 175

W. M. Roberts, *Spatial calcium buffering in saccular hair cells*, Nature, 363 (1993), pp. 74–76. 178

R. Robitaille and M. P. Charlton, *Frequency facilitation is not caused by residual ionized calcium at the frog neuromuscular junction*, Ann. NY Acad. Sci., 635 (1991), pp. 492–494. 188

T. Schikorski and C. F. Stevens, *Quantitative ultrastructural analysis of hippocampal excitatory synapses*, J. Neurosci., 17 (1997), pp. 5858–5867. 175

W.-X. Shen and J. P. Horn, *Presynaptic muscarinic inhibition in bullfrog sympathetic ganglia*, J. Physiol. (Lond.), 491 (1996), pp. 413–421. 185

Z.-H. Sheng, J. Rettig, T. Cook, and W. A. Catterall, *Calcium-dependent interaction of N-type calcium channels with the synaptic core complex*, Nature, 379 (1996), pp. 451–454. 175

Z.-H. Sheng, C. T. Yokoyama, and W. A. Catterall, *Interaction of the syntaxin site of N-type Ca^{2+} channels with the C2B domain of synaptotagmin I*, Proc. Natl. Acad. Sci. USA, 94 (1997), pp. 5405–5410. 175

S. Simon and R. Llinás, *Compartmentalization of the submembrane calcium activity during calcium influx and its significance in transmitter release*, Biophys. J., 48 (1985), pp. 485–498. 173, 175, 176

G. D. Smith, *Analytical steady-state solution to the rapid buffering approximation near an open channel*, Biophys. J., 71 (1996), pp. 3064–3072. 180

G. D. Smith, L. Dai, R. M. Miura, and A. Sherman, *Asymptotic analysis of buffered calcium diffusion near a point source*, SIAM J. Appl. Math., 61 (2001), pp. 1816–1838. 48, 180

G. D. Smith, J. E. Pearson, and J. E. Keizer, *Modeling intracellular calcium waves and sparks*, in Computational Cell Biology, C. P. Fall, E. S. Marland, J. M. Wagner, and J. J. Tyson, eds., Springer, New York, 2002, pp. 198–229. 176, 180

E. F. Stanley, *Decline in calcium cooperativity as the basis of facilitation at the squid giant synapse*, J. Neurosci., 6 (1986), pp. 782–789. 174, 190

———, *Single calcium channels and acetylcholine release at a presynaptic nerve terminal*, Neuron, 11 (1993), pp. 1007–1011. 175

T. C. Südhof, *The synaptic vesicle cycle: A cascade of protein-protein interactions*, Nature, 375 (1995), pp. 645–653. 175

Y. Tang, T. Schlumpberger, T. Kim, M. Lueker, and R. S. Zucker, *Effects of mobile buffers on facilitation: Experimental and computational studies*, Biophys. J., 78 (2000), pp. 2735–2751. 173, 175, 188, 189

M. V. Tsodyks and H. Markram, *The neural code between neocortical pyramidal neurons depends on neurotransmitter release probability*, Proc. Natl. Acad. Sci. USA, 94 (1997), pp. 719–723. 185, 194, 195

J. Wagner and J. Keizer, *Effects of rapid buffer on Ca^{2+} diffusion and Ca^{2+} oscillations*, Biophys. J., 67 (1994), pp. 447–456. 179

J. L. Winslow, S. N. Duffy, and M. P. Charlton, *Homosynaptic facilitation of transmitter release in crayfish is not affected by mobile calcium chelators: implications for the residual ionized calcium hypothesis from electrophysiological and computational analyses*, J. Neurophysiol., 72 (1994), pp. 1769–1793. 173, 188

L.-G. Wu and P. Saggau, *Presynaptic inhibition of elicited neurotransmitter release*, Trends Neurosci., 20 (1997), pp. 204–212. 195

W. M. Yamada and R. S. Zucker, *Time course of transmitter release calculated from simulations of a calcium diffusion model*, Biophys. J., 61 (1992), pp. 671–682. 173, 175, 187

G. W. Zamponi and T. P. Snutch, *Decay of prepulse facilitation of N type calcium channels during G protein inhibition is consistent with binding of a single $G_{\beta\gamma}$ subunit*, Proc. Natl. Acad. Sci. USA, 95 (1998), pp. 4035–4039. 196

R. S. Zucker, *Short-term synaptic plasticity*, Ann. Rev. Neurosci., 12 (1989), pp. 13–31. 193

R. S. Zucker and L. Landò, *Mechanism of transmitter release: voltage hypothesis and calcium hypothesis*, Science, 231 (1986), pp. 574–579. 173

R. S. Zucker and W. G. Regehr, *Short-term synaptic plasticity*, Annu. Rev. Physiol., 64 (2002), pp. 355–405. 173, 184, 193

R. S. Zucker and N. Stockbridge, *Presynaptic calcium diffusion and the time courses of transmitter release and synaptic facilitation at the squid giant synapse*, J. Neurosci., 3 (1983), pp. 1263–1269. 175